LUND UNIVERSITY

Proteins, Blue Copper: Electronic Spectra

Ryde, Ulf; Olsson, Mats H. M.; Roos, Björn O.; Pierloot, Kristine; De Kerpel, Jan O. A.

Published in:
The Encyclopaedia of Computational Chemistry

1998

Document Version:
Peer reviewed version (aka post-print)

Link to publication

Citation for published version (APA):
Ryde, U., Olsson, M. H. M., Roos, B. O., Pierloot, K., & De Kerpel, J. O. A. (1998). Proteins, Blue Copper: Electronic Spectra. In *The Encyclopaedia of Computational Chemistry* (pp. 2255-2270). John Wiley & Sons Inc..

Total number of authors:
5

Creative Commons License:
Unspecified

General rights
Unless other specific re-use rights are stated the following general rights apply:
Copyright and moral rights for the publications made accessible in the public portal are retained by the authors and/or other copyright owners and it is a condition of accessing publications that users recognise and abide by the legal requirements associated with these rights.
• Users may download and print one copy of any publication from the public portal for the purpose of private study or research.
• You may not further distribute the material or use it for any profit-making activity or commercial gain
• You may freely distribute the URL identifying the publication in the public portal

Read more about Creative commons licenses: https://creativecommons.org/licenses/

Take down policy
If you believe that this document breaches copyright please contact us providing details, and we will remove access to the work immediately and investigate your claim.

LUND UNIVERSITY

PO Box 117
221 00 Lund
+46 46-222 00 00

Download date: 05. Dec. 2025

Proteins, Blue Copper: Electronic Spectra

Ulf Ryde, Mats H. M. Olsson and Björn O. Roos
Chemical Centre, Lund, Sweden

Kristine Pierloot and Jan O. A. De Kerpel
University of Leuven, Heverlee-Leuven, Belgium

1 INTRODUCTION

We have in recent years seen an exciting development, where non-empirical quantum chemical methods are used to discuss problems in biochemistry, and we can expect this trend to continue with an increasing pace in the future. The background is the development of methods and computer codes that can deal with larger molecules at reasonable costs. Density functional theory (DFT), in particular, has become a viable tool for studies of ground state properties. In this review we shall give an example of how modern quantum chemical tools can be utilized to analyze the structural and also the spectroscopic properties of a class of copper containing proteins. The DFT method is used to solve structural problems, while the excited states are treated using *ab initio* methods.

The blue copper proteins or cupredoxins constitute a class of copper cysteinate proteins that exhibit a number of specific properties.[1,2] They have an intense color, usually blue, and they have EPR spectra with narrow hyperfine splittings and a varying degree of rhombicity. In addition, the reduction potentials are unusually high. Owing to their characteristic properties, these proteins have been studied extensively for a long time. Crystal structures are known for several blue copper proteins and they show that the copper ion is four- or five-coordinated with a strong bond to a cysteine (Cys) ligand. Two of the other ligands are histidine (His) and the fourth is normally methionine (Met). Large variations are found in the $Cu-S_{Met}$ distance between the different proteins, while the other copper–ligand distances vary much less.

The blue copper proteins serve as charge-transfer proteins. The distorted trigonal geometry assumed by many of them is intermediate between the tetrahedral coordination preferred by Cu(I) and the tetragonal geometry of most Cu(II) complexes. As a result, the change in geometry when Cu(II) is reduced to Cu(I) is small, which gives a small reorganization energy and allows for a high rate of electron transfer. These unusual properties, unknown in inorganic copper chemistry, led to the early proposal that the protein forms a rigid structure, which forces the Cu(II) ion into a coordination geometry more similar to that preferred by Cu(I).[3,4] These suggestions were later extended into general theories for metalloproteins, suggesting that the protein forces the metal center into a catalytically poised state: the entatic state theory[5,6] and the induced rack theory.[7,8] The theoretical results show, however, that no strain is needed to create a trigonal site for Cu(II) when cysteine is one of the coordinating ligands.[9] This will be further discussed below.

Copper sites in proteins have traditionally been classified into three classes: blue type 1 sites (present in the blue copper proteins), normal type 2 sites (tetragonal mononuclear copper sites), and type 3 (spin-coupled pairs of copper ions).[10] The type 1 sites have been further classified as axial or rhombic depending on their EPR (and other spectroscopic) characteristics.[11,12] Plastocyanin (axial) and nitrite reductase (rhombic) are typical examples of type 1 proteins. Proteins with properties intermediate between those of type 1 and type 2 sites have been termed type 1.5.[11,12]

The coordination geometry around Cu(II) is for the axial type 1 proteins close to trigonal. In the rhombic proteins, crystal structures reveal a tetrahedral distortion, with the copper ion about 40 pm out of the His_2Cys plane. Type 2 proteins are tetragonal (with a varying degree of tetrahedral distortion). It has been suggested that this is true also for the cysteinate-containing type 2 sites. In the lack of structures of type 1.5 proteins, it has been suggested that they are even more tetrahedral than the rhombic type 1 sites.

The relation between the structural and spectroscopic properties of the copper cysteinate proteins has been discussed extensively in the literature, based on theoretical studies at different levels of sophistication.[13–16] The strong absorption that occurs around 17000 cm^{-1} in axial type 1 proteins, like plastocyanin, has been shown to arise from a charge-transfer excitation involving the bonding–antibonding pair of π-orbitals that constitute the strong $Cu-S_{Cys}$ bond. In the present review we shall discuss results from a series of recent theoretical studies of the relation between structure and electronic spectra for a number of the copper proteins, ranging from axial (plastocyanin) and rhombic type 1 (nitrite reductase, stellacyanin, cucumber basic protein, and pseudoazurin), to mutants of type 1.5 and 2.[9,15,17,18] Density functional theory (DFT) has been used to determine structures for a series of model compounds, and the electronic spectra have been computed using multiconfigurational SCF methods (CASSCF)[19] and second-order perturbation theory.[20] These studies have given a theoretical explanation for the classification, suggesting that the axial blue type 1 proteins are characterized by a π bond between the copper ion and S_{Cys}, which in turn leads to a trigonal structure of the active site. Small perturbations can change the bond to σ, resulting in a more tetragonal structure and a change in the relative intensity of the two dominant charge-transfer excitations. The varying characteristics of these proteins are thus closely linked to the electronic structure of the $Cu-S_{Cys}$ bond.

2 THEORETICAL METHODS

It is obviously not possible to perform *ab initio* quantum chemical calculations on a whole protein. Therefore models have to be constructed that are as realistic as possible and at the same time computationally tractable. A simple model was used in the work reviewed here. The protein was divided into two parts: the active site, consisting of the copper ion and

the directly coordinated ligands, which was treated quantum mechanically, and the rest of the protein. Most calculations considered only the active site, but some exploratory calculations were made where an array of point charges was used to model the protein. The effects of the protein on the electronic structure in the active site were then simulated through the electric field from the point charges. Several models were tested for the ligands: histidine was modeled by either ammonia or imidazole, cysteine by SH^-, $S(CH_3)^-$, or in some cases by $S(C_2H_5)^-$, methionine by SH_2 or $S(CH_3)_2$, and amide ligands by formaldehyde, formamide, or acetamide. It was shown in the first papers on plastocyanin[9,15] that a converged geometry and spectroscopy for this protein is obtained with imidazole as a model for histidine and with methyl groups on the sulfurs, modeling cysteine and methionine. Smaller models were also used, in particular when discussing trends and differences between related proteins.

The geometries of the active site models were determined using the hybrid density functional method B3LYP, either in the form implemented in the MULLIKEN-2.31h software (MB3LYP)[21] or in GAUSSIAN-94.[22] The semiempirical hybrid density functional methods have been shown to give as good or better geometries as correlated *ab initio* methods for first-row transition metal complexes.[23] However, it was shown in the recent study of plastocyanin[9] that somewhat larger errors (0.05–0.10 Å) are obtained with the B3LYP approach for the Cu–S bonds (both to methionine and cysteine) and these bond distances had to be reoptimized using more accurate *ab initio* methods. The basis set used for Cu in the DFT structure determinations was of the segmented CGTO type (see *Gaussian-type Orbital (GTO)*) with the size 8s5p4d1f.[9,24] 6-31G* basis sets were used for the other atoms (experience shows that geometries obtained with the DFT approach do not change much when the basis set is increased beyond this level[9]).

The electronic spectra were computed using the CASSCF/CASPT2 (second-order *perturbation theory* with a *multiconfigurational* reference state) approach (see ***Complete Active Space Self-consistent Field (CASSCF) Second-order Perturbation Theory (CASPT2)***), which in a number of earlier applications in spectroscopy has been shown to give reliable results for both organic molecules and transition metal complexes.[20] Generally contracted atomic natural orbitals (ANO) type basis sets were used in these calculations.[25] They have the virtue of being compact but at the same time optimized to include as much correlation as possible for a given size. Owing to the size of the systems studied, moderate-size contracted basis sets have been used, including up to f-type functions on Cu and a d-type function on S, but with no polarization functions on C, N, and H. It should be emphasized that such a basis set is on the small side, in particular with the lack of polarization functions on C and N. However, none of the low-lying excited states involve any of these ligands directly. They are either ligand-field transitions located on Cu, or charge transfer between Cu and S. However, as we shall see later, excitations involving charge transfer from the methionine or histidine ligands will be affected by the limitations in the basis set.

The choice of the active orbital space for the CASSCF calculations is a crucial step, and has turned out to be especially difficult in these proteins and similar systems containing a Cu–thiolate bond. From earlier studies it is known that in complexes with copper (and other first-row transition metal ions with many 3d electrons) it is necessary to include in the active space one correlating orbital for each of the doubly occupied 3d orbitals, since the strong radial correlation effects in a crowded 3d shell cannot be accurately described at the second-order level.[20] Therefore the starting active space contains 10 orbitals (3d and 3d′). In addition it is necessary to add the 3p orbitals on S_{Cys} in order to describe correctly the covalent character of the $Cu-S_{Cys}$ bond and also in order to be able to describe charge-transfer states where one electron moves from a sulfur lone-pair orbital to the 3d hole. The final active space will therefore contain 11 or 12 active orbitals. More details will be given in connection with the discussion of the different systems.

The general strategy for CASSCF/CASPT2 calculations of electronic spectra is to first perform a state-averaged CASSCF calculation, where all the excited states of a given symmetry are included in the averaging. This model is also followed here. Some calculations were performed in C_s symmetry, others in C_1. In the former case, a state average was performed separately in the two symmetries A' and A'', in the latter case over all excited states.

The CASSCF wave functions are in the CASPT2 step used as reference functions in a second-order estimate of the remaining dynamical correlation effects. All valence electrons are correlated in this step and also the 3s, 3p shell on copper. Relativistic corrections (Darwin and mass–velocity) were added to all CASPT2 energies. They were obtained at the CASSCF level using first-order perturbation theory.

The CASPT2 calculations were performed with a level-shift added to the zeroth-order Hamiltonian in order to remove intruder states. A series of test calculations had been performed on $Cu(imidazole)_2(SH)(SH_2)^+$ to study the effect of the level-shift on computed excitation energies.[26] It was shown that a level-shift of 0.3 could be used to remove all intruder-state problems, without deteriorating the excitation energies, and this level-shift was used in all calculations. Transition moments were computed using the CAS state-interaction method[27] at the CASSCF level. They were combined with CASPT2 excitation energies to obtain the oscillator strengths. The CASSCF/CASPT2 calculations were performed with the MOLCAS-3.1 quantum chemistry software.[28]

The discussion of the methods given above has been by necessity brief. The interested reader is referred to the quoted literature for more details about the CASSCF/CASPT2 method and its application in spectroscopy.

3 COPPER GEOMETRY IN THE BLUE PROTEINS

3.1 Protein Strain in Blue Copper Proteins

According to the induced rack and the entatic state theories,[6,8] the Cu(II) coordination sphere in the blue copper proteins is strained into a Cu(I)-like structure. Such hypotheses are hard to test experimentally, but with theoretical methods it is quite straightforward. The actual coordination preferences of the copper ion can be determined by optimizing the geometry of the ion and its ligands in vacuum; if the optimized structure is almost the same as in the proteins, strain is most probably of minor importance for the geometry.

The geometry of $Cu(imidazole)_2(SCH_3)(S(CH_3)_2)^+$ was optimized using the MB3LYP method (without any symmetry

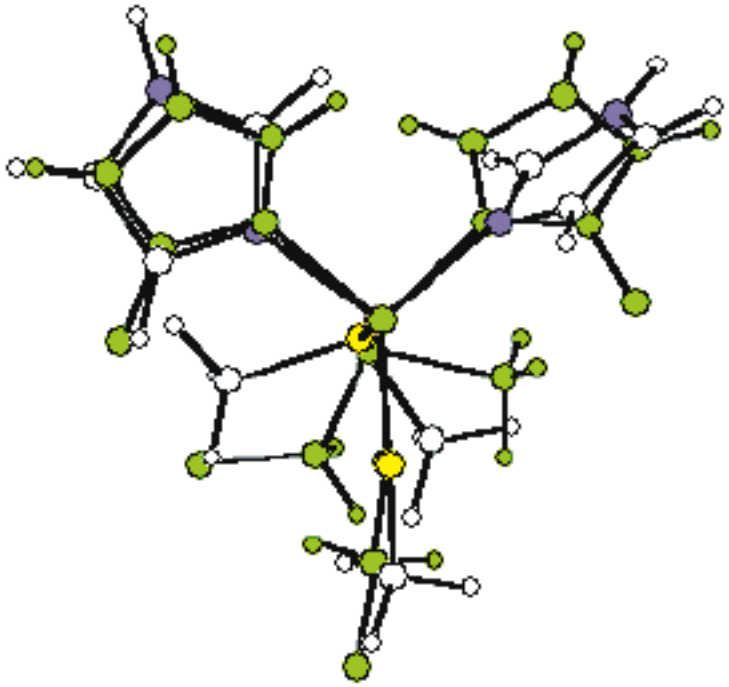

Figure 1 The optimized structure of Cu(imidazole)$_2$(SCH$_3$)(S(CH$_3$)$_2$)$^+$ compared to the crystal structure of oxidized plastocyanin (shaded)[45]

constraints).[9] As can be seen in Figure 1, the optimized geometry is virtually identical to the crystal structure of plastocyanin and other blue copper proteins. The bond lengths to and the bond angles around the copper ion are all well within the range encountered in crystal structures of different blue copper proteins and usually near the experimental average (Table 1); the largest error in the angles is only 5°. The Cu–N bond lengths are excellently reproduced (2 pm error), while the difference in the two Cu–S distances is somewhat larger; the Cu–S_{Cys} bond is 6 pm too long, and the Cu–S_{Met} bond is 15 pm too short. This is mainly due to deficiencies in the theoretical method. If the two distances are optimized with the CASPT2 method, keeping the rest of the geometry fixed, the Cu–S_{Cys} distance decreases by 7 pm and the Cu–S_{Met} distance increases by 7 pm.

The remaining difference in the Cu–S_{Met} distance is due to the extraordinarily shallow potential surface of this bond; the quadratic force constant is only 6 J mol^{-1} pm^{-2}, which is more than four times smaller than for normal metal–ligand bonds. This means that the 8 pm difference between the optimized and experimental Cu–S_{Met} bond length corresponds to less than 0.5 kJ mol^{-1}. In fact, the Cu–S_{Met} bond length may change as much as 50 pm around the minimum at a cost of less than 5 kJ mol^{-1}, which explains why the Cu–S_{Met} bond length varies so widely among blue copper proteins from different organisms.[1,2] Consequently, the bond should be extremely sensitive to the electrostatic properties of the surrounding protein matrix.

The flat potential surface of the Cu–S_{Met} bond is interesting for another reason. It has been suggested that the Cu–S_{Met} bond length is of fundamental importance for the reduction potentials of different blue copper proteins.[29] However, since the experimental range of the Cu–S_{Met} distance corresponds to an energy difference of only 5 kJ mol^{-1}, or 50 mV, this can only explain a minor part of the experimental range of reduction potentials of blue copper proteins, 180–680 mV.[2]

Geometry optimizations of the reduced copper complexes (Table 2) are more complicated, because the lower charge on the copper ion leads to weaker bonds that are very sensitive to electrostatic factors and hydrogen bonds.[9] The optimized structure of Cu(imidazole)$_2$(SCH$_3$)(S(CH$_3$)$_2$) without symmetry is more tetrahedral than the crystal structure of reduced plastocyanin and has too short a Cu–S_{Met} bond length (237 pm). However, if the Cu–S_{Met} bond is fixed to the experimental value (290 pm) and the geometry is reoptimized, a structure is obtained that closely resembles the crystal structure. Moreover, this structure is only 4 kJ mol^{-1} less stable than the fully optimized one, i.e., well within the error limits of the method,

Table 1 Comparison of the Optimized Geometry of Cu(imidazole)$_2$(SCH$_3$)(S(CH$_3$)$_2$)$^+$ and the Crystal Structures of Oxidized Blue Copper Proteins

Structure	Distance to Cu (pm)			Angle subtended at Cu			
	S_{Cys}	N	S_{Met}	N–N	S_{Cys}–N	S_{Cys}–S_{Met}	N–S_{Met}
Calculated	218	204	267	103	120–122	116	94–95
Experimental range	202–221	189–222	262–310	94–133	74–144	102–138	83–120
Experimental average	212	206	283	103	120	111	98

Table 2 Comparison of Two Optimized Geometries of Cu(imidazole)$_2$(SCH_3)($S(CH_3)_2$)$^+$ and the Crystal Structures of Reduced Blue Copper Proteins

Structure	Distance to Cu (pm)			Angle subtended at Cu			
	S_{Cys}	N	S_{Met}	N–N	S_{Cys}–N	S_{Cys}–S_{Met}	N–S_{Met}
Optimal	232	214–215	237	109	105–108	115	107–113
Cu–S_{Met} fixed	227	205–210	290	119	112–120	99	100–101
Experimental range	211–240	203–239	270–315	92–119	108–141	99–114	83–110
Experimental average	218	217	290	103	123	108	97

so it is impossible to decide whether the reduced structure in the blue copper proteins is natural or if it is imposed by the protein, as has been suggested lately.[29]

3.2 Trigonal and Tetragonal Structures

In conclusion, these results lend no support to the suggestion that the blue copper proteins force the metal coordination sphere into an unnatural, Cu(I)-like geometry as the strain hypotheses suggest.[8,6] Why then is the structure of the Cu(II) coordination sphere in the blue copper proteins trigonal while most inorganic Cu(II) complexes assume a tetragonal structure (distorted octahedral or square-planar)? This problem was studied by comparing the geometry, electronic structure, and energetics of a number of small four-coordinate Cu(II) complexes, $Cu^{2+}(NH_3)_3L$, where L is NH_3, OH^-, SH^-, SeH^-, NH_2^-, PH_2^-, OH_2, SH_2, or one of the halogenides.[30]

For most of the complexes, stationary points representing tetragonal as well as trigonal geometries could be found. Interestingly, a vibrational analysis shows that the less stable geometry is always a transition state. This can be rationalized by examining the angle ϕ between the N_1–Cu–N_2 and the N_3–Cu–L (S_{Met}–Cu–S_{Cys} in the proteins) planes. In a square-planar structure, $\phi = 0^\circ$ or 180°, while in an ideal trigonal structure $\phi = 90^\circ$. The trigonal structure can then be viewed as a transition state between two (identical) square-planar structures, and vice versa.

Figure 2 shows the geometry and the electronic structure of these two conformations for $Cu(NH_3)_3(SH)^+$. In the tetragonal geometry, the four lobes of the singly occupied Cu 3d orbital overlap with a lone-pair orbital from each of the four ligands, i.e., all the four ligands make a σ bond to the copper ion. This is in accord with the normal ligand-field view of a d^9 metal ion. In the trigonal geometry, however, one of the ligand orbitals makes instead a π bond to the copper ion. Thus, the orbital overlaps with two lobes of the Cu 3d orbital and the ligand formally occupies two corners in a square coordination, again in accord with the ligand-field view. The fourth ligand cannot then overlap with the singly occupied orbital and has to interact instead with a doubly occupied orbital. Since such an interaction is weaker, it becomes an axial ligand with an enlarged copper distance. Thus, the effective coordination number is decreased, and the three strong ligands in the trigonal complex bind at shorter distances to the copper ion than in the tetragonal complex. This explains the short Cu–S_{Cys} bond in the normal blue copper proteins, together with the fact that a π bond to copper is shorter than the corresponding σ bond.[31–33]

Formally, the $Cu^{2+}(NH_3)_3L$ complexes consist of a Cu(II) ion with nine d electrons and a neutral or negatively charged L-ligand. For three ligands, SeH^-, NH_2^-, and PH_2^-, however, the negative charge on the ligand moves to the copper ion, yielding a Cu(I) ion and an uncharged ligand radical. Since the Cu(I) ion has a full d shell, it prefers a tetrahedral structure and these three ligands give complexes that are strongly tetrahedrally distorted. The thiolate ligand is intermediate: in the $Cu(NH_3)_3(SH)^+$ complex, the electron is delocalized between the copper ion and the thiolate ion. Therefore, both the trigonal and the tetragonal structures are rather tetrahedral, and are in fact quite similar. Naturally, this facilitates electron transfer to and from the complex by reducing the reorganization energy.

The stability of the trigonal and tetragonal geometries varies with the L-ligand. For OH^-, the halogenides, and the uncharged L-ligands, the ground state is tetragonal and the trigonal transition states are found at 34–58 kJ mol^{-1} higher (CASPT2) energy. For SeH^-, the structure is instead trigonal, and the tetragonal geometry is a 18 kJ mol^{-1} less stable transition state. For $Cu(NH_3)_3(SH)^+$, $Cu(NH_3)_3(NH_2)^+$, and $Cu(NH_3)_3(PH_2)^+$, finally, the two geometries have the same energy within a few kJ mol^{-1}.

Some models of the blue copper proteins were also studied. It turned out that these models may assume either a trigonal or a tetragonal geometry (although not always for the same complex). A characteristic difference between the two types of geometry is that the tetragonal structure has a longer Cu–S_{Cys} bond (223 pm) and a shorter Cu–S_{Met} bond (242 pm) than the trigonal structure (218 and 267 pm, respectively, see Table 3). Morover, the ϕ angle is smaller in the tetragonal structure (62◦ compared with 90°), and the two largest angles around the copper ion in the trigonal structure are between S_{Cys} and the two histidine nitrogen atoms, while in the tetragonal structure the two largest angles are between two distinct pairs of atoms (S_{Cys}–Cu–N and S_{Met}–Cu–N). Most interestingly, these structural differences remind us of the differences in the crystal structure of plastocyanin and nitrite reductase. More detailed investigations (see below) show that this is not accidental; plastocyanin and more generally the axial type 1 copper proteins have a trigonal structure with a π bond between copper and the thiolate ligand, while the so-called rhombic type 1 copper proteins (e.g., nitrite reductase) have a tetragonal structure with mainly σ bonds to the copper ion.

Why do some proteins assume a trigonal structure while others assume a tetragonal structure? This is primarily due to the fact that the energy difference between the two structures is small, less than 15 kJ mol^{-1} in all models examined. Furthermore, the potential surface is so flat that the topology is extremely sensitive to the chemical properties of the ligands and to the environment.[17] It turns out that the relative stability of the two structures varies when the ligand models are modified. With $Cu(NH_3)_2(SH)(SH_2)^+$

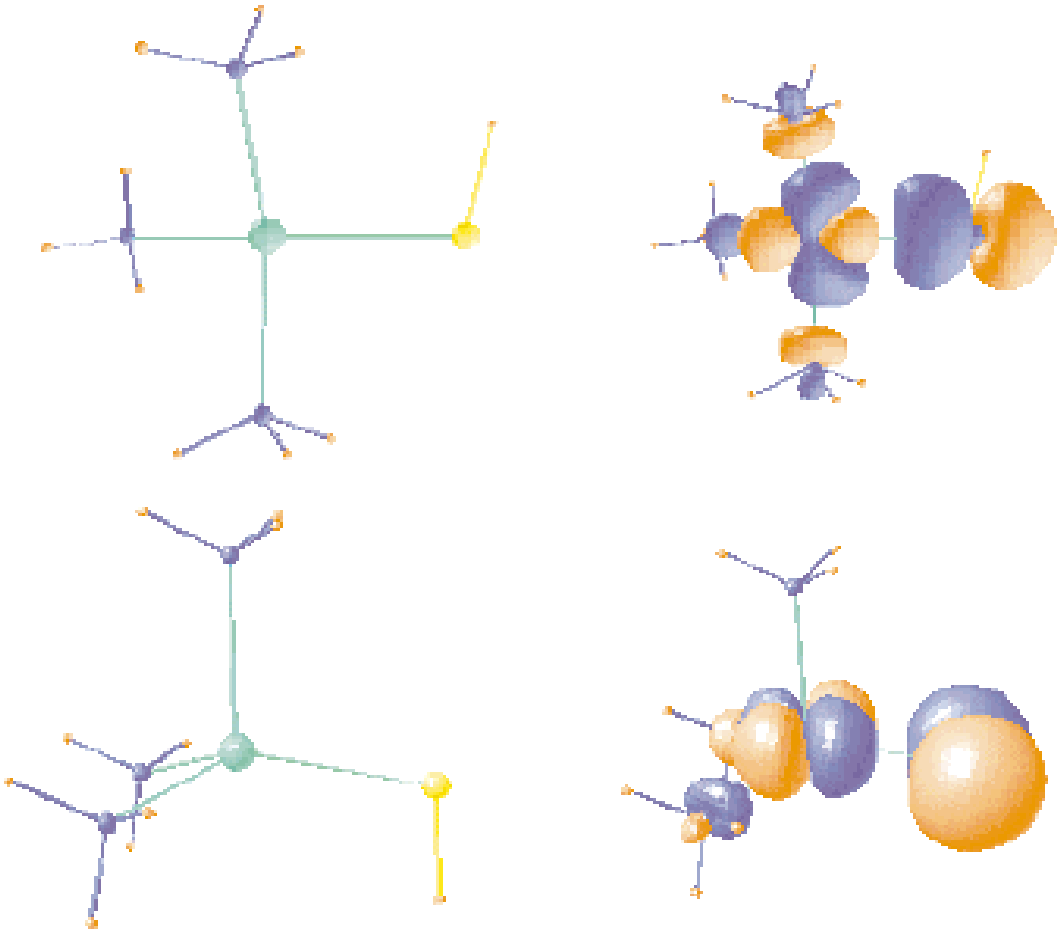

Figure 2 The geometry and the singly occupied orbital of $Cu(NH_3)_3(SH)^+$ for (a) the tetragonal structure and (b) the trigonal structure[30]

Table 3 Comparison of the Best Models of Plastocyanin and Nitrite Reductase, $Cu(imidazole)_2(SCH_3)(S(CH_3)_2)^+$, and $Cu(imidazole)_2(SH)(S(CH_3)_2)^+$ Optimized by the MB3LYP Method, and Two Crystal Structures of the Same Proteins (PDB1PCL and PDB1NIC). It Should be Noted that the Uncertainty in the Crystal Structures is about 7 pm and 7°

Model	Distance to Cu (pm)			Angle subtended at Cu				
	S_{Cys}	N	S_{Met}	N–N	S_{Cys}–N	S_{Cys}–S_{Met}	N–S_{Met}	ϕ
Plastocyanin model	218	204	267	103	120–122	116	94–95	90
Nitrite reductase model	223	205–206	242	100	97–141	103	95–126	62
Plastocyanin crystal	207	191–206	282	97	121–132	110	88–101	82
Nitrite reductase crystal	218	202–203	265	100	103–133	106	88–131	57

and $Cu(imidazole)_2(SH)(SH_2)^+$, the trigonal structure is most stable. However, if methionine is modeled by $S(CH_3)_2$, the tetragonal structure is most stable, while the trigonal structure becomes a transition state. If a methyl group is added also to the cysteine model, the trigonal structure is again stabilized and becomes the ground state. With the most realistic model $Cu(imidazole)_2(SCH_3)(S(CH_3)_2)^+$, it was not possible to find a minimum corresponding to nitrite reductase. Instead, in addition to the trigonal ground state, a structure was found with a short Cu–S_{Met} bond and a Cu–S_{Cys} bond that was mainly of π character. The structure is probably best described as (chiefly) trigonal with one of the imidazoles as an axial ligand.

Altogether, this illustrates that the equilibrium between the two structures is extremely sensitive to changes in the ligand models. Consequently, very small changes in the protein environment (hydrogen bonds or the electrostatic field around the copper ion) may stabilize either structure, or perhaps also stabilize some intermediate structures.

It should also be pointed out that there exists a number of other possible conformations of the blue copper models. All plastocyanin models described up to now have a S_{Met}–Cu–S_{Cys}–C_{Cys} dihedral angle around 0°. This is close to the angle encountered in the protein. However, under vacuum more stable structures are found if this dihedral angle is changed to 180°. This is because the latter structures are stabilized by weak CH–S_{Cys} hydrogen bonds. In the proteins much better hydrogen-bond donors are available that stabilize the former conformation. In the nitrite reductase

models, the S_{Met}–Cu–S_{Cys}–C_{Cys} dihedral angle is intermediate (50–80°) and only one conformation exists. Other structures can be obtained when other dihedral angles are changed. They are often three-coordinate, since the Cu–S_{Met} bond is rather weak.

Calculations of EPR parameters were also performed on some of the complexes.[17] Experimental EPR spectra are either axial ($g_x = g_y$; axial type 1 copper proteins) or rhombic (other blue copper proteins). The results indicate that the geometry is more important than the electronic structure for the rhombicity of the spectrum: the optimized trigonal structure of $Cu(imidazole)_2(SCH_3)(S(CH_3)_2)^+$ and the crystal structure of plastocyanin both give an axial spectrum, while both the crystal structure of nitrite reductase and the other optimized model of $Cu(imidazole)_2(SCH_3)(S(CH_3)_2)^+$ give a rhombic spectrum, although the latter structure is mainly π bonded with an axial imidazole ligand. The reason for this behavior has not yet been fully explored.

The existence of trigonal and tetragonal structures seems to be general for copper–cysteine complexes. An illustrative example is the geometry of the catalytic metal ion in copper-substituted alcohol dehydrogenase (the native enzyme contains zinc). Here, the copper ion is coordinated by two cysteine residues, one histidine residue, and a ligand from the solution. A recent crystal structure with dimethylsulfoxide as the fourth ligand shows a trigonal structure with dimethylsulfoxide as an axial ligand at a large distance (319–345 pm). Preliminary calculations[32] show that the electronic structure of such complexes is very similar to the traditional blue copper proteins. The His ligand and one of the Cys ligands make σ bonds to the copper ion, while the other S_{Cys} atom makes a π bond to copper. Thus, the two cysteine ligands are not equivalent; the π bonded ligand has a shorter Cu–S_{Cys} bond and larger angles to the other ligands compared with the σ bonded ligand (217 and 225 pm, respectively).

Furthermore, tetragonal structures may also be obtained for models of Cu–alcohol dehydrogenase. When the fourth ligand is uncharged, they are less stable than the corresponding trigonal complexes (in accord with the crystal structure). However, with OH^- (which is involved in the reaction mechanism of the native enzyme) as the fourth ligand, the tetragonal structure becomes the most stable structure. This may explain some of the spectral shifts that are observed experimentally when the coenzyme or the ligands are changed.[34]

3.3 Different Types of Copper Protein

On the basis of the electronic, resonance Raman, and EPR spectra, the cysteine-containing copper proteins have been divided into four groups: axial type 1 (e.g., plastocyanin and azurin), rhombic type 1 (e.g., nitrite reductase, cucumber basic protein, pseudoazurin, and stellacyanin), type 1.5, and type 2 copper proteins. For the different type 1 proteins, numerous crystal structures are available, and they have been interpreted as trigonal for the axial proteins and tetrahedrally distorted trigonal for the rhombic proteins.[11,12] On the basis of the theoretical results, such an interpretation is a bit misleading. It is true that the rhombic proteins are slightly more tetrahedral than the axial proteins, with the copper distance out of the N_2S_{Cys} plane ranging between 24–63 pm, compared with 0–32 pm in the axial proteins. However, the main difference between these proteins is in the electronic structure, with a Cu–S_{Cys} π bond in the axial proteins but mainly a σ bond in the rhombic proteins. Thus, the axial proteins are trigonal, while the rhombic proteins have (tetrahedrally distorted) *tetragonal* structures. This can be quantified by the ϕ angle; in the axial proteins it is 76–89°, while it is 56–82° for the rhombic proteins.

The only exception from this scheme is stellacyanin, which has a ϕ angle (82–86°) well within the range of the axial type 1 proteins but with spectroscopic characteristics typical for a rhombic type 1 protein. The reason is probably that this protein has another axial ligand, a glutamine residue that makes a much shorter bond to copper than the normal methionine ligand. Recent theoretical calculations[35] show that the structure is mainly trigonal, but the short bond to the axial ligand (around 224 pm) leads to a Cu–S_{Cys} bond that contains a mixture of π and σ interactions.

It is notable that the axial proteins are a rather homogeneous group, while the rhombic proteins seem to be more heterogenous. Nitrite reductase is the extremum with a very short Cu–S_{Met} bond (258 pm), a rather long Cu–S_{Cys} bond (217 pm), low ϕ angles (56–65°), and typical tetragonal angles (the largest angles between distinct pairs of atoms). This is also reflected in the spectral properties. The other proteins (pseudoazurin and cucumber basic protein) are more intermediate, however. They have a longer Cu–S_{Met} bond (261–269 pm), a shorter Cu–S_{Cys} bond (214–215 pm), intermediate ϕ angles (70–74°), and less clear relations between the angles around the copper ion.

Type 1.5 and type 2 copper–cysteinate proteins do not exist in nature; they have all been constructed by site directed mutagenesis on different proteins, mainly azurin or Cu,Zn-superoxide dismutase. For the type 1.5 proteins, a recent crystal structure is available, the azide derivative of the Met121-Ala azurin mutant.[36] In addition, preliminary results on the Met121-His azurin mutant, another type 1.5 protein, have also been presented.[37]

Before the crystal structures were published, it was suggested that the type 1.5 proteins should be more tetrahedral than the other types.[12] However, the crystal structures do not support such a suggestion; the distance of the copper ion to the plane consisting of the three strongest ligand atoms is 15–44 pm (average 29 pm) in the type 1.5 structures, which is significantly less than for the rhombic type 1 proteins (average 42 pm). Considering the theoretical result, it would be more probable that the type 1.5 proteins have a more flattened tetragonal structure, i.e., a structure with a lower ϕ angle. Owing to the limited accuracy of the crystal structures, it is hard to decide whether this really is so; the type 1.5 crystal structures have $\phi = 46$–76° (average 62°) which is less than for all rhombic type 1 proteins (70–82°), except nitrite reductase (56–65°). It is notable that $Cu(NH_3)_3(SH)^+$, which is a simple model of the type 1.5 Met121-His azurin mutant has $\phi = 53$–54°. Most probably, the spectral characteristics of the type 1.5 proteins are an effect both of the flattened tetragonal structure and the presence of a fourth strong ligand (in type 1.5 proteins the weak methionine ligand is replaced by a stronger ligand).

It has been suggested that the type 2 copper cysteinate proteins are tetragonal with four strong ligands in a near-square-planar geometry.[11,12] This is in accord with theory, indicating that type 2 sites are obtained when ϕ is less than about 45°. This idea was tested by optimizing a tentative model of a

type 2 protein, the His117Gly azurin mutant (without extraneous ligands).[38] Two water molecules were assumed to come in from the solution and become strong equatorial ligands in an octahedral coordination with the normal methionine thioether and the backbone amide oxygen atoms as axial ligands. As expected this gave rise to an octahedral structure with the four strong ligands in an approximate square plane ($\phi = 25^{\circ}$) and with an increased Cu–S_{Cys} distance (229 pm). Interestingly, the structure remained even if the axial ligands were removed. As will be discussed below, the spectrum of this model was of type 2 character.

In summary, the theoretical studies show that the fundamental difference between the different types of copper protein is between the axial and the rhombic type 1 proteins, i.e., between a tetragonal σ bonded structure and a trigonal π bonded structure. For the other groups there is no distinct difference; the three tetragonal types seem to differ mainly by the extent of tetrahedral distortion and the number and properties of the ligands. Evidently, the type 1 proteins arise when there are three strong ligands and one weak ligand (thioether or carbonyl). The type 1.5 proteins probably arise when all four ligands are strong, while it seems likely that the nearly square-planar type 2 cysteinate proteins arise when there are four strong ligands and one or two weaker axial ligands.

3.4 The Role of the Protein

In conclusion, the blue copper proteins seem to have constructed a metal coordinating site that minimizes the electron-transfer reorganization energy, not by straining the geometry, but by an appropriate choice of metal ligands, viz. ligands that are a compromise between those preferred by the Cu(I) and Cu(II) ions. In particular, the cysteine thiolate ligand seems to be crucial, giving rise to rather tetrahedral structures (either trigonal or tetragonal). Moreover, the methionine thioether ligand gives a very soft bond that may easily be manipulated by the electrostatic potential and the local dielectric environment around the metal and that can change considerably with little expense of energy.

Of course, this does not mean that the protein is unimportant for the structure of the active site in the blue copper proteins. A significant role of the protein is to restrict the number of ligands of the copper ion. Cu(I) complexes are usually four-coordinate and tetrahedral, while Cu(II) complexes normally are more or less six-coordinated (distorted octahedral). In fact, the unusual cupric structure in the blue copper proteins seems to be partly due to the simple fact that the copper ion is four-coordinated without any further axial ligands; most optimized copper cysteinate models are far from square-planar unless the number of ligands is more than five.

Other functions of the protein are also conceivable. Evidently, the protein may change almost freely between the different type 1 structures owing to the extremely flat potential surface. Furthermore, the protein forms a protected environment that prohibits the contact between two copper–thiolate units (thereby inhibiting the homeolysis to Cu(I) and disulfide) and it tunes the reduction potential. However, this is not a special property of the blue copper proteins, but instead an inevitable effect of any protein, presenting an ordered array of charges and dipoles and a dielectric milieu widely different from water solution.

4 ELECTRONIC SPECTROSCOPY OF COPPER CYSTEINATE PROTEINS

The hallmark of cupredoxins, leading to their description as blue or type 1 copper proteins, is the presence in their electronic spectrum of an intense ($\varepsilon_{max} = 3000–6000\ M^{-1}\ cm^{-1}$) absorption band around 600 nm. It is this spectral feature that distinguishes them from the 'normal' or type 2 copper proteins, the spectrum of which only contains a number of much weaker ($\varepsilon = 100\ M^{-1}cm^{-1}$) ligand-field transitions in the same region.[39] However, also within the class of type 1 proteins, variations exist. In addition to the prominent peak at 600 nm, a feature at 460 nm is observed in all spectra with an intensity varying between different proteins.[40,41] Thus the axial type 1 proteins, like plastocyanin and azurin, show only a little absorption in the 460 nm region, while the 460 nm band becomes much more prominent in rhombic type 1 proteins, like pseudoazurin, cucumber basic protein, and stellacyanin. The increasing intensity of the 460 nm band in the rhombic proteins goes together with a decrease in intensity of the 600 nm band, and in fact the consistency of the sum of $\varepsilon_{460\ nm}$ and $\varepsilon_{600\ nm}$ has been noted.[40] A limiting case is nitrite reductase from *Achromobacter cycloclastes*. The intensity of the 600 nm absorption peak is in this enzyme reduced by a factor 3 compared with the classic proteins, and the 460 nm absorption has actually become the more intense, resulting in a green color of the enzyme. No natural proteins exist in which the blue band is even further reduced, but by site-directed mutagenesis a number of mutants (mostly of azurin) have been constructed in which only the second band is present, shifted to around 410 nm, giving them a yellow-orange color. Based on the analogy of their EPR characteristics with the normal type 2 copper proteins (which indicates a similar tetragonal copper ligand surrounding) these mutants have been classified as 'type 2'. The classification of mutants with intermediate spectroscopic characteristics as type 1.5 then follows naturally.

Apart from these two characteristic peaks, several additional weak features have been discerned in the visible to near-infrared region of the spectra of some type 1 copper proteins. Based on different types of spectroscopic analyses (including the absorption of polarized light by oriented single crystals) and with the help of the density functional $X\alpha$ scattered wave method, Solomon and co-workers[13] discovered and assigned a total of nine different absorption bands in the spectrum of plastocyanin. They proposed that the 600 nm (16 700 cm^{-1}) band is due to a charge transfer from a cysteine sulfur p orbital with π overlap to a Cu orbital, and that the 460 nm (21 390 cm^{-1}) band is predominantly His $\rightarrow$ Cu charge-transfer in character. An additional feature at 18 700 cm^{-1} was assigned to a charge transfer from the so-called S_{Cys} pseudo-σ orbital. The analysis also included the ligand-field states and a number of higher-lying charge-transfer states. A similar study was performed recently on the spectrum of nitrite reductase.[16] A total of seven bands was found in this case. The 600 nm blue band was given the same assignment as in plastocyanin, while the most prominent 460 nm (21 900 cm^{-1}) band was assigned to an excitation from the S_{Cys} pseudo-σ orbital. All transitions were found at significantly higher wavenumbers than in plastocyanin, indicating an increased ligand-field strength, which was related to the considerably flattened copper coordination geometry in nitrite reductase.

Recently, the results of the first *ab initio* CASPT2 study of the spectrum of plastocyanin were reported.[15] A number of different model compounds of the type Cu(II)N_2(SC)(SM) were used, with N = NH_3 or imidazole modeling histidine, SC = SH^-, SCH_3^-, or $SC_2H_5^-$ as a model for cysteine, and SM = SH_2 or $S(CH_3)_2$ modeling methionine. In this review we shall limit the discussion, in Section 4.1, to the results obtained for Cu(imidazole)$_2$(SCH_3)($S(CH_3)_2$)$^+$, the smallest model for which consistent results were obtained. In Section 4.2 a much smaller model will be used, Cu(NH_3)$_2$(SH)(SH_2)$^+$, for a qualitative description of the structure–spectroscopy relation in the different types of proteins. Finally, in Section 4.3, the effect of the surrounding crystal will be examined for a number of type 1 proteins. The model used in this case is Cu(imidazole)$_2$(SH)(SH_2)$^+$.

4.1 The Electronic Spectrum of Cu(imidazole)$_2$(SCH_3)($S(CH_3)_2$)$^+$ as a Model for Plastocyanin

The actual conformation of the active site in plastocyanin does not contain any symmetry (owing to the tilted orientation of the imidazoles). Still, the N–Cu–N and S_{Met}–Cu–S_{Cys} planes are approximately perpendicular, so that a reasonable approximation of the actual copper coordination geometry in plastocyanin could be obtained by optimizing (using the MB3LYP method) the structure of Cu(imidazole)$_2$(SCH_3)($S(CH_3)_2$)$^+$ in C_s symmetry, thus both reducing the computational effort and simplifying the classification of the different excited states.

Calculations of electronic spectra using the CASSCF/CASPT2 approach are normally based on one set of CASSCF calculations for each symmetry, where the molecular orbitals are optimized with respect to the average energy for all electronic states under consideration. One CASPT2 calculation is then performed for each state. This approach has been used successfully in a large number of applications. It ensures that all electronic states are orthogonal to each other and noninteracting (in contrast to a calculation which optimizes each state separately). Here, two separate state-averaged CASSCF calculations were performed, one for each possible symmetry, A' or A'', and using equal weights for each of the states included. In each CASSCF calculation, 13 electrons were correlated in an active space of 12 orbitals, consisting of the Cu 3d and 3d′ orbitals, and two ligand orbitals belonging to the symmetry representation used in the calculation. This way, a total of nine states, four of A' symmetry and five of A'' symmetry, could be calculated, including the different ligand-field states and the lowest ligand-to-metal charge-transfer states.

The results are shown in Table 4. The different excited states can be labeled by their characteristic singly occupied molecular orbital, i.e., the orbital involved in the excitation. These orbitals are shown in Figure 3, and their main atomic orbital components are listed in Table 4. The corresponding orbital for the X^2A'' ground state is shown at the bottom of the figure. As one can see, this orbital is strongly delocalized over the Cu–S_{Cys} bond. It involves a π antibonding interaction of the Cu $3d_{xy}$ and S_{Cys} $3p_y$ orbitals, combined with a much weaker σ antibonding interaction with the two N ligands, whose positions in the equatorial plane are such that a perfect σ overlap with the two remaining lobes of the Cu $3d_{xy}$ orbital is obtained. As discussed above, this ground-state electronic structure of the C_S Cu(imidazole)$_2$(SCH_3)($S(CH_3)_2$)$^+$ model offers an explanation for the stability of the trigonal Cu(II) coordination surrounding in plastocyanin. The Cu–S_{Cys} σ interaction also has a strongly covalent character, as is obvious from the composition of the singly occupied orbital in the first excited state (a^2A'), where we find a σ antibonding combination of the Cu $3d_{x^2-y^2}$ and S_{Cys} $3p_x$ orbitals. The calculated excitation energy for this state is 4 302 cm^{-1}, which explains the appearance of the low-lying band at 5000 cm^{-1} in the plastocyanin spectrum. Between 10 000 and 14 000 cm^{-1} three bands are found in the experimental spectrum, corresponding to the calculated states b^2A', b^2A'', and c^2A'. From the composition of the corresponding singly occupied orbitals it is clear that the states concerned can be labeled as genuine ligand-field states, with the electron hole localized in the Cu $3d_{z^2}$, $3d_{yz}$, and $3d_{xz}$ orbitals, respectively.

The dominant blue band, appearing at 16 700 cm^{-1} in the experimental spectrum of plastocyanin, was calculated at 15 933 cm^{-1} and corresponds to the c^2A'' state. As can be seen from Figure 3, the corresponding singly occupied orbital is the bonding counterpart of the Cu–S_{Cys} π antibonding orbital containing the hole in the ground state. The extremely good overlap between both orbitals immediately explains the large absorption intensity of the corresponding excitation. Even if

Table 4 The Spectrum of Cu(imidazole)$_2$(SCH_3)($S(CH_3)_2$)$^+$ (in cm^{-1}), Calculated at the CASPT2 level

State	Main character of the singly occupied orbital[a]	ΔE(osc. str.)	exp.[13]
X^2A''	51% Cu3d$_{xy}$ + 3% Cu3d$_{yz}$ + 45% S_{Cys} + 1% Im		
a^2A'	3% Cu3d$_{z^2}$ + 19% Cu3d$_{xz}$ + 44% Cu3d$_{x^2-y^2}$ + 5% Cu4s + 3% Cu4p + 1% S_{Met} + 25% S_{Cys}	4 302	5 000
b^2A'	85% Cu3d$_{z^2}$ + 9% Cu3d$_{x^2-y^2}$ + 5% S_{Met} + 1% Im	11 647	10 800(.0031)
b^2A''	19% Cu3d$_{xy}$ + 74% Cu3d$_{yz}$ + 6% S_{Cys}	14 243(.0091)	12 800(.0114)
c^2A'	3% Cu3d$_{z^2}$ + 69% Cu3d$_{xz}$ + 27% Cu3d$_{x^2-y^2}$	14 890	13 950(.0043)
c^2A''	29% Cu3d$_{xy}$ + 24% Cu3d$_{yz}$ + 46% S_{Cys} + 1% Im	15 933(.1500)	16 700(.0496) 18 700(.0048)
d^2A'	4% Cu3d$_{z^2}$ + 11% Cu3d$_{xz}$ + 20% Cu3d$_{x^2-y^2}$ + 4% Cu4s + 3% Cu4p + 58% S_{Cys}	18 861(.0005)	21 390(.0035)
e^2A'	5% Cu3d$_{z^2}$ + 2% Cu4s + 2% Cu4p + 91% S_{Met}	31 264	23 440(.0030)
d^2A''	100% Im	34 992	32 500

[a]The coordinate system is defined as follows: the copper ion is at the origin, the z axis is along the Cu–S_{Met} bond, and the Cu–S_{Cys} bond is situated in the xz plane.

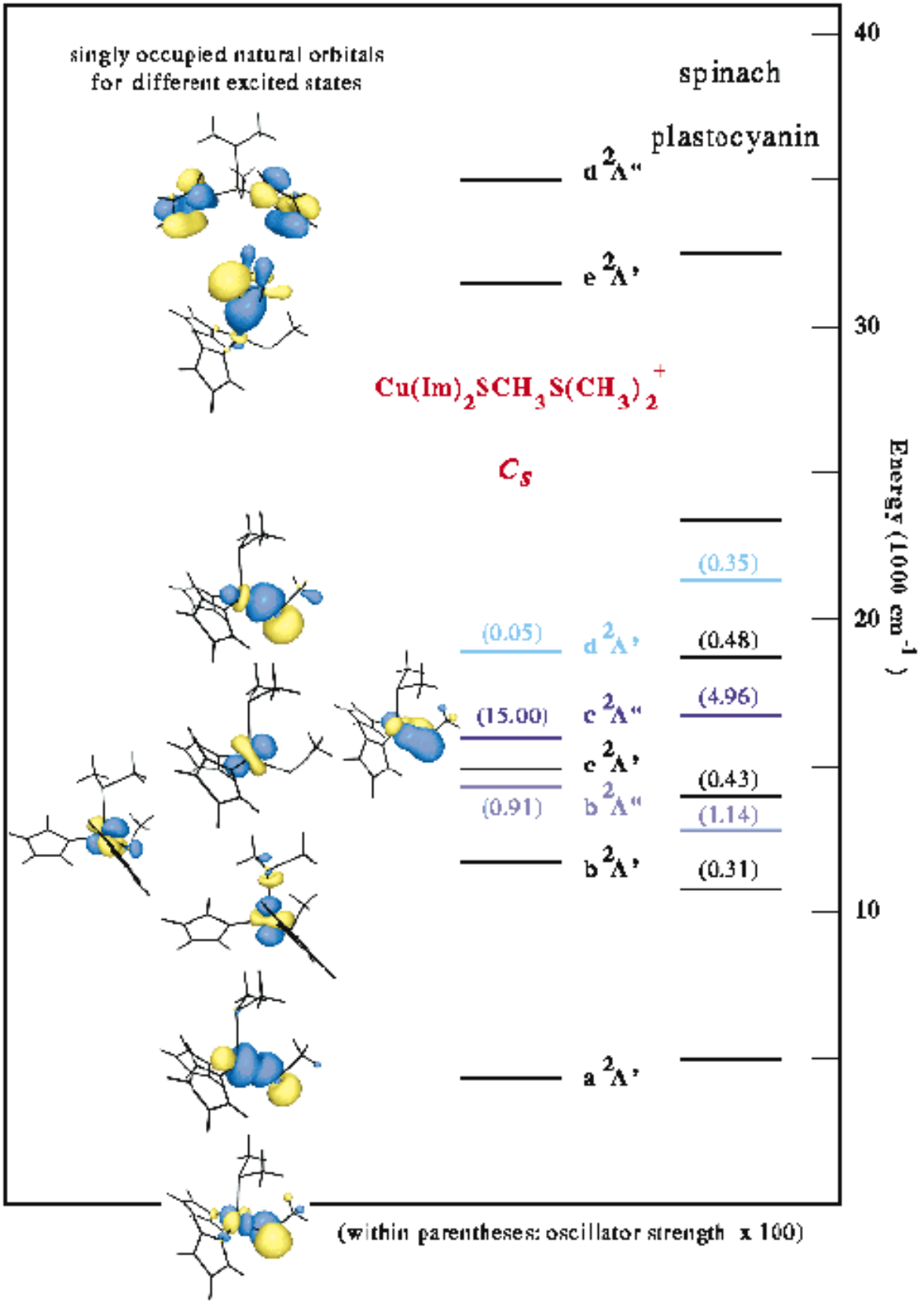

Figure 3 Comparison between the calculated spectrum of the (MB3LYP) optimized C_s model Cu(imidazole)$_2$(SCH$_3$)(S(CH$_3$)$_2$)$^+$ and the experimental spectrum of spinach plastocyanin[13]

this transition formally can be labeled as a $S_{Cys} \rightarrow Cu$ charge-transfer excitation, the actual amount of charge transferred is practically zero. The presence of a definite amount of S_{Cys} $3p_\pi$ character in the predominantly Cu $3d_{yz}$ orbital of the b^2A'' state is also notable. This mixing creates a significant intensity for the $X^2A'' \rightarrow b^2A''$ ligand-field excitation, which is in fact responsible for the second most intense band in the plastocyanin spectrum.

Below 30 000 cm^{-1} only one further excited state was found (d^2A'), whereas the experimental spectrum[13] exhibits three bands at 18 700 cm^{-1}, 21 390 cm^{-1}, and 23 440 cm^{-1}. The singly occupied orbital in the d^2A' state is the σ bonding combination of Cu $3d_{x^2-y^2}$ and S $3p_x$, corresponding to the antibonding orbital of the a^2A' state. This orbital is denoted as the S_{Cys} pseudo-σ orbital by Gewirth and Solomon,[13] who assign the band at 18 700 cm^{-1} in the experimental spectrum as the corresponding excitation to the d^2A' state, and the higher-lying bands at 21 390 cm^{-1} and 23 440 cm^{-1} as charge-transfer excitations from imidazole and methionine respectively. The calculated CASPT2 excitation energy for the d^2A' state in the present $Cu(imidazole)_2(SCH_3)(S(CH_3)_2)^+$ model, 18 861 cm^{-1}, is also closest to the band at 18 700 cm^{-1}, making it tempting to accept Solomon's assignment. However, a more detailed analysis of the spectra of several other model compounds at different geometries[15] indicates that the excitation energy of the d^2A' state (and also the c^2A'' state) in fact strongly depends on the metal–ligand distances, and in particular the Cu–S_{Cys} distance. For example, by changing the latter distance from the MB3LYP optimized value used here to the experimental distance in the plastocyanin crystal structure, the excitation energy of the d^2A' state is raised by more than 2000 cm^{-1}, so that it actually comes closer to the band at 21 390 cm^{-1}. Furthermore, the band at 21 390 cm^{-1} corresponds to the second characteristic peak at 460 nm, which becomes much more intense in other type 1 proteins, and there is strong experimental evidence,[40,42] that this transition involves the cysteine sulfur rather than imidazole: the resonance Raman excitation profiles associated with the 600 nm and 460 nm bands in a series of blue copper proteins indicate that both electronic transitions are primarily $S_{Cys} \rightarrow Cu$ in character. It is therefore more reasonable to assign the 21 390 cm^{-1} to the d^2A' state, as is done in Table 4. As concerns the assignment of the band at 23 440 cm^{-1} as a charge-transfer originating from methionine, we tend to agree with Solomon, even if we predict a much higher excitation energy for this charge-transfer excitation in the present $Cu(imidazole)_2(SCH_3)(S(CH_3)_2)^+$ model; the CASPT2 excitation for this state (e^2A') is 31 264 cm^{-1}. However, again structural effects are very important. In this case the Cu–S_{Met} bond length has the largest effect: increasing this distance by 30 pm (toward the experimental value) reduces the calculated excitation energy by about 4000 cm^{-1}.[15] Another source of uncertainty is connected to the limited size of the basis sets used for the CASPT2 calculations. Test calculations on smaller model systems have indicated that the use of small basis sets affects the results for the e^2A' state considerably more than for the other states, and that the use of larger basis sets could decrease the excitation energy of this state by up to 3000 cm^{-1}.[15] The combined effect of both corrections (structure and basis sets) would bring the calculated excitation energy of the e^2A' state to within good agreement with the band at 23 440 cm^{-1} .

Finally, at 32 500 cm^{-1} another weak band appears in the plastocyanin spectrum, which should be attributed to the d^2A'' state, with a singly occupied orbital consisting of an almost pure imidazole π orbital. The calculated excitation energy, 34 992 cm^{-1}, is satisfactory, and confirms the assignment by Gewirth and Solomon[13] of the highest band in the plastocyanin UV–visible spectrum to an imidazole $\rightarrow$ Cu charge-transfer excitation.

The discussion above shows that the assignment of an electronic spectrum based on theoretical results is far from trivial. Both theory and experiment have inherent uncertainties, which must be balanced against each other. We have noticed that the theoretical results will depend on the correlation treatment (CASPT2), the basis set, the model used for the active site, and the structure. We shall discuss some of these effects in more detail below. Also the experimental data are ambigous. The bands are broad and overlapping and a Gaussian resolution is based on assumptions about the number of bands, and is often not unique. It is not certain that all bands are of electronic origin, the sample may not be pure, etc. We notice that one of the bands in the plastocyanin spectrum has been left unassigned (18 700 cm^{-1}). With the data at hand, it is rather meaningless to speculate about the origin of this band. It is clear, however, that it appears neither in the electronic spectrum of the model compound, nor in the experimental spectrum of nitrite reductase.

4.2 Correlation Between the Structure and Spectroscopic Properties of Different Types of Copper Cysteinate Protein

An important issue in the reviewed work has been the relation between the structure and the spectroscopic characteristics in the different cysteinate-containing copper enzymes. This was studied for $Cu(NH_3)_2(SH)(SH_2)^+$ by calculating the spectrum at different values of the angle ϕ between the S_{Cys}–Cu–S_{Met} and N–Cu–N planes.[17] The calculations were performed on partially optimized structures, obtained in two steps. In a first step, structures were obtained with the B3LYP method by constraining only the angle ϕ and optimizing all other geometrical parameters. In a second step, all parameters were kept fixed at their B3LYP values, except for the Cu–S_{Cys} and Cu–S_{Met} distances, which were reoptimized using CASPT2 (remember that significant deviations from the experimental results were obtained for these parameters at the B3LYP level of theory). The CASPT2 calculations were performed with an active space of 11 electrons in 11 orbitals (Cu 3d, 3d′ and the highest S_{Cys} 3p orbital). All valence but not the Cu 3s, 3p electrons were correlated in the CASPT2 step, in order to keep basis set superposition errors to a minimum.

For the CASPT2 calculations of the spectra, the active space was extended with the second S_{Cys} 3p orbital. No symmetry was used in the calculations, and all states were included in one state-averaged CASSCF calculation. With 13 electrons in 12 orbitals, seven states, consisting of all ligand-field states as well as the two $S_{Cys} \rightarrow Cu$ charge-transfer states, could be included in the calculations.

The results are shown in Table 5. Spectra were calculated for a selected number of ϕ angles, ranging from the 'ideal' trigonal structure ($\phi = 90^\circ$) to a strictly square-planar structure ($\phi = 0^\circ$). The composition of the singly occupied molecular

Table 5 Calculated spectrum of $Cu(NH_3)_2(SH)(SH_2)^+$ as a Function of the Angle ϕ between the S_{Cys}-Cu-S_{Met} and N-Cu-N planes[a]

		$\phi = 90°$	$\phi = 80°$	$\phi = 70°$	$\phi = 60°$	$\phi = 45°$	$\phi = 30°$	$\phi = 0°$		
a^2A'	(Cu-S)σ^* → (Cu-S)π^*	4 313(.0000)	3 655(.0001)	3 833(.0001)	5 416(.0000)	7 456(.0001)	9 131(.0000)	10 583(.0000)	a^2A''	(Cu-S)π^* → (Cu-S)σ^*
b^2A'	$Cu3d_{z^2}$ → (Cu-S)π^* LF	12 842(.0000)	12 334(.0000)	12 287(.0005)	13 785(.0009)	16 097(.0016)	17 256(.0014)	18 164(.0013)	b^2A'	$Cu3d_{xz}$ → (Cu-S)σ^* LF
c^2A'	$Cu3d_{xz}$ → (Cu-S)π^* LF	14 774(.0000)	14 252(.0001)	14 423(.0006)	15 243(.0006)	16 661(.0001)	18 757(.0006)	20 005(.0007)	c^2A'	$Cu3d_{y^2}$ → (Cu-S)σ^* LF
b^2A''	$Cu3d_{yz}$ → (Cu-S)π^* LF	14 861(.0019)	14 206(.0023)	14 766(.0013)	16 023(.0011)	17 519(.0012)	18 868(.0007)	20 824(.0000)	b^2A''	$Cu3d_{yz}$ → (Cu-S)σ^* LF
c^2A''	(Cu-S)π → (Cu-S)π^* CT	15 042(.1225)	14 575(.1053)	14 981(.0441)	15 453(.0296)	16 432(.0191)	17 670(.0108)	18 866(.0007)	c^2A''	(Cu-S)π → (Cu-S)σ^* CT
d^2A'	(Cu-S)σ → (Cu-S)π^* CT	22 036(.0008)	21 427(.0158)	21 412(.0902)	21 638(.1128)	22 053(.1305)	22 440(.1432)	22 527(.1560)	d^2A'	(Cu-S)σ → (Cu-S)σ^* CT

[a]The axes are chosen such that S_{Met} remains on the z axis and S_{Cys} in the xz plane along the entire rotation path, while the plane containing the two NH_3 groups is rotated.

orbital in the ground and excited states of the trigonal structure is similar to the composition shown in Table 4 for the $Cu(imidazole)_2(SCH_3)(S(CH_3)_2)^+$ model of plastocyanin (see also the orbital plots in Figure 3), and only the main component of the Cu 3d orbitals is shown on the left side of Table 5. In the square-planar structure, all ligands are situated in the xz plane, and the ground state singly occupied orbital is a σ antibonding orbital between the Cu $3d_{z^2-x^2}$ orbital and the four ligands, containing a considerable amount (21%) of S_{Cys} $3p_\sigma$ character and a much smaller amount of S_{Met} and NH_3 character, 3% and 2%, respectively. Both the trigonal and square-planar structures possess C_s symmetry, and the different excited states are labeled according to their symmetry representation on both sides of the table.

Looking at the spectrum of the trigonal structure first, we recognize the main characteristics of the plastocyanin spectrum. The c^2A'' state, giving rise to the dominant 'blue' band, is calculated at 15 042 cm^{-1}, while the second $S_{Cys} \rightarrow$ Cu charge-transfer band is found at 22 036 cm^{-1} with little or no intensity. As for $Cu(imidazole)_2(SCH_3)(S(CH_3)_2)^+$ the only ligand-field state giving rise to a transition with significant intensity is b^2A''. In the square-planar structure, the situation is reversed. The ground state is X^2A', and the d^2A' state, corresponding to the Cu–S_{Cys} $\sigma \rightarrow \sigma^*$ excitation, has become by far the most intense, while the c^2A'' state has almost completely vanished. The intensity of the ligand-field states also reflects the change in ground state: the intensity of the d^2A'' state has dropped to zero, while the b, c^2A' states now gain intensity from the presence of a small amount of S_{Cys} $3p_\sigma$ character in the corresponding singly occupied orbitals. All excitation energies have increased in the square-planar structure compared with the trigonal structure. The strongest increase, around 6000 cm^{-1}, is found for the first excited state and the ligand-field states, reflecting the stronger ligand-field exerted in the square-planar structure, with four instead of three strongly bound ligands. The excitation energies of the two charge-transfer states are also raised, but less. For the c^2A'' state an increase of 3800 cm^{-1} is found, while the d^2A' state is raised by less than 500 cm^{-1}.

Even if the calculations were performed on a simple model, the results presented in Table 5 would nicely reflect the structure–electronic spectroscopy relationship between the different types of copper cysteinate proteins. The copper coordination geometry of axial type 1 proteins is close to trigonal, and their spectroscopic characteristics are reflected by the results obtained for $\phi = 90^\circ$. Rhombic type 1 proteins like pseudoazurin and cucumber blue protein on the other hand typically have ϕ angles between 70 and 80°. As can be seen from Table 5, even at such a small deviation from orthogonality, the transition to the d^2A' state has already gained significant intensity due to mixing of σ character into the ground-state singly occupied orbital. The largest deviation from orthogonality within the type 1 copper proteins is found for nitrite reductase: in the *Achromobacter cycloclastes* nitrite reductase crystal structure, $\phi = 56$–65°.[43] Accordingly, the most important spectroscopic characteristics of this protein are reflected in the results obtained for $\phi = 60^\circ$. The spectrum of nitrite reductase will be discussed in more detail in the next section. At this point we already note that all calculated excitation energies are higher than for $\phi = 90^\circ$, in agreement with the shifts found in the experimental nitrite reductase spectrum compared with plastocyanin.[16] The redistribution of the intensities of the two charge-transfer bands between $\phi = 90^\circ$ and $\phi = 60^\circ$ is also notable, with the second transition being the most intense at $\phi = 60^\circ$. This is in accord with the green color of nitrite reductase.

The intensity of the blue band further decreases as the structure is even more flattened, and the results obtained for the smallest ϕ angles in Table 5 can to a first approximation be used to mimic the properties of type 2 copper–cysteinate (mutant) proteins, with their yellow color and gradually more tetragonal structure. A more accurate description of these mutant proteins is obtained by substituting the appropriate ligands in the $Cu(NH_3)_2(SH)(SH_2)^+$ model. Table 6 shows the results obtained for the spectrum of two such models: $Cu(NH_3)_3(SH)^+$, serving as a model for the Met121His azurin mutant, and $Cu(NH_3)(OH_2)_2(SH)^+$ as a tentative model for His117Gly(H_2O) azurin, a mutant obtained by replacing one histidine by two water molecules.[12,38] MB3LYP optimized structures were used, with only the Cu–S_{Cys} distance reoptimized at the CASPT2 level. The optimum $Cu(NH_3)_3(SH)^+$ structure has an angle $\phi = 53$–54° (depending on which of the two S_{Cys}–Cu–N planes is considered), while $Cu(NH_3)(OH_2)_2(SH)^+$ is considerably more flattened, with $\phi = 28$–29°. This conforms with the classification of Met121His azurin as type 1.5 and His117Gly(H_2O) azurin as type 2. The difference between both types is also reflected in the calculated spectra. The excitation from the (Cu–S)σ bonding orbital is by far the most intense in both cases, but more in $Cu(NH_3)(OH_2)_2(SH)^+$ than in $Cu(NH_3)_3(SH)^+$, while the intensity of the blue band decreases in the same order. Finally, it is also notable that the calculated (Cu–S)$\sigma \rightarrow$ (Cu–S)σ^* excitation energy is considerably (more than 1000 cm^{-1}) higher for $Cu(NH_3)(OH_2)_2(SH)^+$ than for $Cu(NH_3)_3(SH)^+$ or $Cu(NH_3)_2(SH)(SH_2)^+$. This is in agreement with the experimentally observed blue shift of the second $S_{Cys} \rightarrow$ Cu charge-transfer band when going from type 1 to type 2 copper cysteinate proteins, from 460 nm (21 800 cm^{-1}) to 410 nm (24 400 cm^{-1}).[12]

Table 6 Calculated Spectrum of $Cu(NH_3)_3(SH)^+$ and $Cu(NH_3)(OH_2)_2(SH)^+$ as Models for Type 1.5 and Type 2 Copper Cysteinate Proteins Respectively

$Cu(NH_3)_3(SH)^+$	$Cu(NH_3)(OH_2)_2(SH)^+$	
7 400(.0000)	9 501(.0000)	(Cu–S)$\pi^* \rightarrow$ (Cu–S)σ^*
14 053(.0001)	17 292(.0010)	Cu3d $\rightarrow$ (Cu–S)σ^* LF
14 617(.0000)	18 187(.0001)	Cu3d $\rightarrow$ (Cu–S)σ^* LF
15 288(.0020)	18 414(.0019)	Cu3d $\rightarrow$ (Cu–S)σ^* LF
16 086(.0157)	16 212(.0029)	(Cu–S)$\pi \rightarrow$ (Cu–S)σ^* CT
22 559(.1340)	23 634(.1728)	(Cu–S)$\sigma \rightarrow$ (Cu–S)σ^* CT

4.3 Influence of the Structure and Surrounding Crystal on the Electronic Spectra of Type 1 Copper Proteins

All spectroscopic results reported in this review so far were obtained on isolated model systems, using quantum chemically optimized structures. The fact that the quality of these results is high enough to provide an explanation of the main spectroscopic characteristics of the different types of protein is very satisfactory, and points to the absence of any crucial role played by the surrounding protein. However, at the same time, it has also become clear during the course of calculations on different model systems that the calculated CASPT2 results for the spectra quite strongly depend on the geometry used.[15] Of particular importance are the Cu–S_{Cys} and Cu–S_{Met} distances, which are also the two geometrical parameters that give the largest uncertainties in the B3LYP geometry optimizations.

In order to obtain more accurate results, an obvious solution would be to calculate the spectra using experimental crystal structures whenever available. However, the experimental structures also contain appreciable uncertainties that may seriously affect the results obtained for the spectra, a point that will be illustrated in the results below.

When using crystal structures it also becomes possible to include the effect of the surrounding protein on the spectrum. Calculations along these lines were performed for several type 1 proteins, and the results obtained for three representative cases, plastocyanin, cucumber basic protein, and nitrite reductase, are presented in Table 7. All three enzymes have the same Cu(II) ligands, two histidine, one methionine, and one cysteine. The calculations were performed on Cu(imidazole)$_2$(SH)$(SH_2)^+$ without symmetry, using the respective crystal geometries[44] of the three proteins, truncated by hydrogen atoms placed at standard bond lengths in the direction of the removed carbons. The effect of the surrounding protein and solvent molecules was estimated using a point-charge model, as described in Ref. 15. The results obtained with and without surrounding crystal are compared in Table 7. They clearly show that the effect of the crystal cannot be neglected. The general trends are the same for the three proteins, and can be related to the character of the transitions: the excitation energy of the two $S_{Cys} \rightarrow$ Cu charge-transfer states increases considerably, by up to 2500 cm^{-1}, while the ligand-field excitations, which involve an appreciable charge flow from Cu to S_{Cys}, decrease by almost 2000 cm^{-1}. A considerably smaller effect is found for the lowest transition, which is essentially a transition within the Cu–S_{Cys} bond. It is also notable that the surrounding crystal reduces all oscillator strengths by a factor of up to 1.75.

As concerns the relative intensity of the two $S_{Cys} \rightarrow$ Cu charge-transfer states, the trends observed experimentally for the different proteins are qualitatively reproduced, with the second transition possessing very little intensity in plastocyanin but becoming significantly stronger in cucumber basic protein and actually winning the battle in nitrite reductase. The quantitative trends observed in the excitation energies are not reproduced by these calculations however, at least not between plastocyanin and nitrite reductase. Instead of the increase found for all transitions between nitrite reductase and plastocyanin in Solomon's analysis of both spectra,[16] a decrease is found, amounting to more than 3000 cm^{-1} for the blue band. The latter is calculated at 16 970 cm^{-1} in plastocyanin, close to the experimental excitation energy of 16 700 cm^{-1}. However, in nitrite reductase the calculated result is 13 863 cm^{-1}, which is almost 4000 cm^{-1} lower than the experimental band at 17 550 cm^{-1}. Yet, the correct trends were reproduced by the calculations on the small Cu$(NH_3)_2$(SH)$(SH_2)^+$ model in the previous section. This fact makes it doubtful whether the large error found here can be entirely traced back to deficiencies in the theoretical approach. Rather, we expect that it is at least partly caused by errors in the crystal structures.

In order to check this, a second set of calculations was performed on the spectra of plastocyanin and nitrite reductase, using the same crystal structures, but replacing the Cu–S_{Met} and Cu–S_{Cys} bond distances by their CASPT2 value as optimized for the Cu$(NH_3)_2$(SH)$(SH_2)^+$ model (see previous section) at ϕ angles 82° and 61° (the angles found in the crystal structures), respectively. For plastocyanin this leads to a lengthening of the Cu–S_{Cys} bond, from 2.07 Å to 2.10 Å, while in nitrite reductase the corresponding bond is shortened, from 2.18 Å to 2.14 Å. The differences for the Cu–S_{Met} bonds are larger and in both cases this bond is shortened: from 2.82 Å to 2.71 Å in plastocyanin, and from 2.65 Å to 2.41 Å in nitrite reductase. Table 8 contains the results of this second set of calculations, together with the experimental band positions found in both spectra. The results shown were obtained for the naked Cu(imidazole)$_2$(SH)$(SH_2)^+$ cluster and were corrected afterwards for the effect of the surrounding crystal using the results of Table 7 (no correction was applied to the oscillator strengths, however).

The effect of the change in geometry is profound. For plastocyanin, increasing the Cu–S_{Cys} distance by 0.03 Å results in a decrease of the excitation energies of both charge-transfer states by 1316 cm^{-1} and 1766 cm^{-1}, while in nitrite reductase increases of 1926 cm^{-1} and 1689 cm^{-1} are found when the same bond length is decreased by 0.04 Å. The effect of the simultaneous changes in the Cu–S_{Met} bond length is expected to be limited. Similar, but smaller effects are found for the four lowest states in the spectra: all excitation energies decrease for plastocyanin and increase for nitrite reductase between Tables 7 and 8. As a result, with the (CASPT2) optimized

Table 7 Comparison between the Electronic Spectra of Different Type 1 Copper Proteins

	Plastocyanin		Cucumber basic protein		Nitrite reductase		
	no crystal	with crystal	no crystal	with crystal	no crystal	with crystal	
(Cu–S)$\sigma^* \rightarrow$ (Cu–S)π^*	5 411(.0000)	4 836(.0000)	4 861(.0001)	5 540(.0000)	3 487(.0000)	4 391(.0000)	(Cu–S)$\pi^* \rightarrow$ (Cu–S)σ^*
Cu3$d_{z^2} \rightarrow$ (Cu–S)π^* LF	14 475(.0000)	12 537(.0000)	12 878(.0003)	11 291(.0001)	12 870(.0009)	11 618(.0006)	Cu3$d_{z^2} \rightarrow$ (Cu–S)σ^* LF
Cu3$d_{yz} \rightarrow$ (Cu–S)π^* LF	15 356(.0028)	13 556(.0028)	14 699(.0022)	13 252(.0012)	13 344(.0002)	11 595(.0000)	Cu3$d_{yz} \rightarrow$ (Cu–S)σ^* LF
Cu3$d_{xz} \rightarrow$ (Cu–S)π^* LF	15 084(.0004)	13 235(.0003)	14 586(.0001)	13 002(.0001)	13 860(.0025)	12 657(.0014)	Cu3$d_{xz} \rightarrow$ (Cu–S)σ^* LF
(Cu–S)$\pi \rightarrow$ (Cu–S)π^* CT	15 948(.1189)	16 970(.1032)	13 535(.0674)	15 860(.0662)	12 331(.0342)	13 863(.0323)	(Cu–S)$\pi \rightarrow$ (Cu–S)σ^* CT
(Cu–S)$\sigma \rightarrow$ (Cu–S)π^* CT	22 093(.0010)	23 156(.0014)	20 505(.0387)	23 001(.0272)	19 049(.0865)	20 772(.0749)	(Cu–S)$\sigma \rightarrow$ (Cu–S)σ^* CT

Table 8 Comparison between the Calculated and Experimental Spectra of Plastocyanin and Nitrite Reductase. Calculations Performed with $Cu-S_{Cys}$ and $Cu-S_{Met}$ Distances, as optimized (CASPT2) for the Small $Cu(NH_3)_2(SH)(SH_2)^+$ Model

	Plastocyanin		Nitrite reductase		
	calc.	exp.	exp.	calc.	
$(Cu-S)\sigma^* \rightarrow (Cu-S)\pi^*$	4 363(.0001)	5 000(.0000)	5 600(.0000)	4 408(.0000)	$(Cu-S)\pi^* \rightarrow (Cu-S)\sigma^*$
$Cu3d_{z^2} \rightarrow (Cu-S)\pi^*$ LF	11 645(.0000)	10 800(.0031)	11 900(.0026)	12 329(.0003)	$Cu3d_{z^2} \rightarrow (Cu-S)\sigma^*$ LF
$Cu3d_{yz} \rightarrow (Cu-S)\pi^*$ LF	12 981(.0025)	12 800(.0114)	13 500(.0086)	12 872(.0004)	$Cu3d_{yz} \rightarrow (Cu-S)\sigma^*$ LF
$Cu3d_{xz} \rightarrow (Cu-S)\pi^*$ LF	12 671(.0002)	13 950(.0043)	14 900(.0101)	13 873(.0028)	$Cu3d_{xz} \rightarrow (Cu-S)\sigma^*$ LF
$(Cu-S)\pi \rightarrow (Cu-S)\pi^*$ CT	15 654(.1162)	16 700(.0496)	17 550(.0198)	15 789(.0325)	$(Cu-S)\pi \rightarrow (Cu-S)\sigma^*$ CT
$(Cu-S)\sigma \rightarrow (Cu-S)\pi^*$ CT	21 974(.0012)	21 390(.0035)	21 900(.0299)	22 461(.1192)	$(Cu-S)\sigma \rightarrow (Cu-S)\sigma^*$ CT

values for both Cu–S distances, the experimentally observed trends in the excitation energies between nitrite reductase and plastocyanin are well reproduced. Except for the second ligand-field state, all calculated excitation energies are higher for nitrite reductase than for plastocyanin, with differences up to 1200 cm^{-1} (the experimental differences range between 500 and 1100 cm^{-1}). The overall agreement between the calculated and experimental excitation energies is also satisfactory. The largest error is still found for the blue band in nitrite reductase, but it is reduced to less than 1800 cm^{-1}, within the uncertainty of the CASPT2 method.

In summary, it is clear that both the effects of geometry changes and the surrounding protein on the calculated transition energies are substantial, and the uncertainties connected with the former as well as the approximate model used for the latter may seriously affect the theoretical results obtained for the spectra. All CASPT2 results obtained in this and the previous sections are therefore afflicted with some uncertainties. However, it was demonstrated that the quality of these results is high enough to provide an understanding of the spectroscopic characteristics of the different types of cysteine-containing copper proteins, in relation to their structure. For the first time, it has been possible to obtain an *ab initio* description of the spectra of these chromophores inside a protein, with an accuracy that is far superior to the results obtained before with semiempirical methods, such as the $X\alpha$ method used by Solomon[13,16] or the recent CNDO/S calculations by Larsson et al.[14] on the spectrum of plastocyanin.

5 CONCLUDING REMARKS

This article has reviewed some recent theoretical work on the relation between structural and spectroscopic properties of the blue copper proteins. The intention has been to illustrate how contemporary quantum chemical methods can be used to study and solve a non-trivial biochemical problem. The accuracy of the methods we use today is such that once the answer has been obtained we can with confidence use them to explain the chemical properties. It is, for example, clear that the DFT calculations of the geometry preferences of the four-coordinated Cu(II) ion explain the structural properties of the active site without invoking the rest of the protein more than marginally, that is, no strain energy is needed to arrive at the trigonal structure. In contrast, the results show that with some ligands, the structure in the protein is also the preferred structure under vacuum. The calculations also showed that the potential surface is very shallow, which then results in small reorganization energies during the redox process.

It is now well known that the B3LYP implementation of DFT will yield accurate structure data for many systems, also those involving transitions metal ions. We have also seen, however, that this semiempirical approach is not capable of accurately predicting the bond length between the copper ion and the sulfur ligands. This is probably, at least partly, due to the fact that the empirical parameters in the B3LYP procedure have not used data involving atoms from the second and third row. Thus, some care has to be taken when using the results obtained from the DFT calculations, especially for soft bonds with a shallow potential surface. One might argue that, if the potential surface is shallow, the requirements for the accuracy of the bond distance are not so strict. We have also seen, however, that the spectroscopic properties are sensitive to the structure (meaning of course that the potential surfaces for the excited states are not equally shallow).

Multiconfigurational second-order perturbation theory has been used to compute the electronic spectra of the different proteins. The results are surprisingly accurate and can be used to explain in rather great detail the relation between the structural and spectroscopic properties. However, one should bear in mind all the uncertainties that are inherent in the comparison of the theoretical and experimental data. The CASPT2 method itself has an uncertainty, by now well documented, in the computed excitation energies of up to 2500 cm^{-1}. To this should be added the basis set effects, which as we saw, were especially crucial for the charge-transfer states involving the methionine and histidine ligands. In addition, there is the effect of the protein and solvent, which was described by a rather primitive point-charge model. The significant influence that the protein has on the spectroscopic properties is most interesting and calls for a more accurate investigation. Preliminary results indicate that most of the effect comes from a few atoms near S_{Cys}. Thus, the calculated effect of the protein strongly depends on the charge of these atoms. However, it also means that it would be enough to improve the model of a few residues near the copper site. For example, these residues might be modeled by higher electrostatic moments calculated from the conformation assumed (and the environment encountered) in the protein.

However, even if the theoretical data were perfect, the comparison with and interpretation of the experimental findings would still be difficult due to the large uncertainties of the data. Protein structural data have relatively large error bars for bond distances. It is clear from the discussion above that the use of theoretical structure data leads to a more consistent interpretation of the spectroscopic data. This is maybe not so surprising, since we expect the theoretical structures to be more accurate. Also the interpretation of the spectroscopic data

is ambiguous, as they are based on a Gaussian fit, which has to assume the number of bands in the spectrum. We saw that for plastocyanin a weak band (at 18 700 cm^{-1}) has no counterpart in the theoretical spectrum and is most probably an artifact.

We have illustrated in this review that it is possible to use advanced quantum chemical methods to discuss and analyze experimental data for macromolecules. Not only has it been possible to study the ground state properties (which is today done for a large number of biochemical systems), but it has also been possible to achieve a detailed understanding of the spectroscopic data and their relation to the nature and the geometrical arrangement of the ligands in the active site for a series of related proteins.

6 RELATED ARTICLES

Combined Quantum Mechanics and Molecular Mechanics Approaches to Chemical and Biochemical Reactivity; Complete Active Space Self-consistent Field (CASSCF) Second-order Perturbation Theory (CASPT2); Density Functional Applications; Density Functional Theory (DFT), Hartree–Fock (HF), and the Self-consistent Field; Density Functional Theory Applications to Transition Metal Problems; Quantum Mechanical/Molecular Mechanical (QM/MM) Coupled Potentials; Spectroscopy: Computational Methods; Transition Metals: Applications.

7 REFERENCES

1. A. G. Sykes, *Adv. Inorg. Chem.*, 1990, **36**, 377–408.
2. E. T. Adman, *Adv. Protein Chem.*, 1991, **42**, 145–197.
3. B. G. Malmström, in 'Oxidases and Related Redox Systems', eds., T. E. King, H. S. Mason, and M. Morrison, Wiley, New York, 1965, pp. 207–216.
4. R. J. P. Williams, in 'Molecular Basis of Enzyme Action and Inhibition', ed. P. A. E. Desnuelle, Pergamon, Oxford, 1963 pp. 133–149.
5. B. L. Vallee and R. J. P. Williams, *Proc. Natl. Acad. Sci. USA*, 1968, **59**, 498–505.
6. R. J. P. Williams, *Eur. J. Biochem.*, 1995, **234**, 363–381.
7. H. B. Gray and B. G. Malmström, *Comments Inorg. Chem.*, 1983, **2**, 203–209.
8. B. G. Malmström, *Eur. J. Biochem.*, 1994, **223**, 207–216.
9. U. Ryde, M. H. M. Olsson, K. Pierloot, and B. O. Roos, *J. Mol. Biol.*, 1996, **261**, 586–596.
10. M. W. G. de Bolster, R. Cammack, D. N. Coucouvanis, J. Reedijk, and C. Veeger, *J. Biol. Inorg. Chem.*, 1996, **1**, G29.
11. G. W. Canters and G. Gilardi, *FEBS Lett.*, 1993, **325**, 39–48.
12. C. R. Andrew, H. Yeom, J. S. Valentine, B. G. Karlsson, N. Bonander, G. van Pouderoyen, G. W. Canters, T. M. Loehr, and J. Sanders-Loehr, *J. Am. Chem. Soc.*, 1994, **116**, 11489–11498.
13. A. A. Gewirth and E. I. Solomon, *J. Am. Chem. Soc.*, 1988, **110**, 3811–3819.
14. S. Larsson, A. Broo, and L. Sjölin, *J. Phys. Chem.*, 1995, **99**, 4860–4865.
15. K. Pierloot, J. O. A. De Kerpel, U. Ryde, and B. O. Roos, *J. Am. Chem. Soc.*, 1997, **119**, 218–226.
16. L. B. LaCroix, S. E. Shadle, Y. Wang, B. A. Averill, B. Hedman, K. O. Hodgson, and E. I. Solomon, *J. Am. Chem. Soc.*, 1996, **118**, 7755–7768.
17. K. Pierloot, J. O. A. De Kerpel, M. H. M. Olsson, U. Ryde, L. Eriksson, and B. O. Roos, *J. Am. Chem. Soc.*, 1998, **120**, submitted.
18. M. H. M. Olsson, U. Ryde, B. O. Roos, and K. Pierloot, *J. Biol. Inorg. Chem.*, 1998, **3(2)**, in press.
19. B. O. Roos, in 'Advances in Chemical Physics. *Ab Initio* Methods in Quantum Chemistry - II', ed. K. P. Lawley, John Wiley, Chichester, 1987, Chap. 69, pp. 399–445.
20. B. O. Roos, K. Andersson, M. P. Fülscher, P.-Å. Malmqvist, L. Serrano-Andrés, K. Pierloot, and M. Merchán, in 'Advances in Chemical Physics: New Methods in Computational Quantum Mechanics, Vol. XCIII', eds., I. Prigogine and S. A. Rice, Wiley, New York, 1996, pp. 219–331.
21. J. E. Rice, H. Horn, B. H. Lengsfiels, A. D. McLean, J. T. Carter, E. S. Replogle, L. A. Barnes, S. A. Maluendes, G. C. Lie, M. Gutwski, W. E. Rude, S. P. A. Sauer, R. Lindh, K. Andersson, T. S. Chevalier, P. O. Widmark, D. Bouzida, G. Pacansky, K. Singh, C. J. Gillan, P. Carnevali, W. C. Swope, and B. Liu, 'Mulliken^{TM} Version 2.25b', internal release, IBM Corporation, Almaden, 1995.
22. M. J. Frisch, G. W. Trucks, H. B. Schlegel, P. M. W. Gill, B. G. Johnson, M. A. Robb, J. R. Cheeseman, T. Keith, G. A. Petersson, J. A. Montgomery, K. Raghavachari, M. A. Al-Laham, V. G. Zakrzewski, J. V. Ortiz, J. B. Foresman, J. Cioslowski, B. B. Stefanov, A. Nanayakkara, M. Challacombe, C. Y. Peng, P. Y. Ayala, W. Chen, M. W. Wong, J. L. Andres, E. S. Replogle, R. Gomperts, R. L. Martin, D. J. Fox, J. S. Binkley, D. J. DeFrees, J. Baker, J. P. Stewart, M. Head-Gordon, C. Gonzalez, and J. A. Pople, 'Gaussian 94, Revision D.1', Gaussian, Inc., Pittsburgh, PA, 1995.
23. A. Ricca and C. W. Bauschlicher, *J. Phys. Chem.*, 1994, **98**, 12899–12903.
24. A. Schäfer, H. Horn, and R. Ahlrichs, *J. Chem. Phys.*, 1992, **97**, 2571–2577.
25. K. Pierloot, B. Dumez, P.-O. Widmark, and B. O. Roos, *Theor. Chim. Acta*, 1995, **90**, 87–114.
26. B. O. Roos, K. Andersson, M. P. Fülscher, L. Serrano-Andrés, K. Pierloot, M. Merchán, and V. Molina, *J. Mol. Struct. (Theochem)*, 1996, **388**, 257–276.
27. P.-Å. Malmqvist and B. O. Roos, *Chem. Phys. Lett.*, 1989, **155**, 189–194.
28. K. Andersson, M. P. Fülscher, G. Karlström, R. Lindh, P.-Å. Malmqvist, J. Olsen, B. O. Roos, A. J. Sadlej, M. R. A. Blomberg, P. E. M. Siegbahn, V. Kellö, J. Noga, M. Urban, and P.-O. Widmark, 'MOLCAS Version 3', Department of Theoretical Chemistry, Chemical Center, University of Lund, P.O.B. 124, S-221 00 Lund, Sweden, 1994.
29. J. A. Guckert, M. D. Lowery, and E. I. Solomon, *J. Am. Chem. Soc.*, 1995, **117**, 2817–2844.
30. M. H. M. Olsson, U. Ryde, B. O. Roos, and K. Pierloot, *J. Biol. Inorg. Chem.*, 1998, **3(2)**, in press.
31. K. Pierloot, B. Dumez, and L. G. Vanquickenborne, unpublished results, 1997.
32. A. C. Borin, M. H. M. Olsson, U. Ryde, B. O. Roos, and K. Pierloot, 'The geometry and electronic spectrum of Cu-substituted alcohol dehydrogenase'. To be published, 1998.
33. M. H. M. Olsson, A. C. Borin, U. Ryde, B. O. Roos, and K. Pierloot, 'A quantum chemical investigation of CuSH'. To be published, 1998.
34. E. Cedergren-Zeppezauer, personal communication, 1997.
35. J. O. A. De Kerpel, K. Pierloot, U. Ryde, and B. O. Roos, A theoretical study of the structural and spectroscopic properties of stellacyanin. To be published, 1998.
36. L.-C. Tsai, N. Bonander, K. Harata, G. Karlsson, T. Vänngård, V. Langer, and L. Sjölin, *Acta Crystallogr.*, 1996, **D52**, 950–958.
37. S. J. Kroes, C. R. Andrew, J. Sanders-Loehr, and G. W. Canggers, *J. Inorg. Biochem.*, 1995, **59**, 661.
38. T. den Blaauwen, C. W. G. Hoitinink, G. W. Canters, J. Han, T. M. Loehr, and J. Sanders-Loehr, *Biochemistry*, 1993, **32**, 12455–12464.

39. A. B. P. Lever, 'Inorganic Electronic Spectroscopy', Elsevier, Amsterdam, 1984.
40. J. Han, T. M. Loehr, Y. Lu, J. S. Valentine, B. A. Averill, and J. Sanders-Loehr, *J. Am. Chem. Soc.*, 1993, **115**, 4256–4263.
41. Y. Lu, J. A. Roe, E. B. Gralla, and J. S. Valentine, in 'Bioinorganic Chemistry of Copper', eds., K. D. Karlin and Z. Tyeklár, Chapman & Hall, New York, 1993, pp. 64–77.
42. J. Sanders-Loehr, in 'Bioinorganic Chemistry of Copper', eds., K. D. Karlin and Z. Tyeklár, Chapman & Hall, New York, 1993, pp. 51–63.
43. E. T. Adman, J. W. Godden, and S. Turley, *J. Biol. Chem.*, 1995, **270**, 27458–27474.
44. The following crystal structures were used: poplar plastocyanin at 1.3 Å resolution (PDB file 1PLC),[45] nitrite reductase from *Achromobacter cycloclastes* at 1.9 Å resolution (PDB file 1NIC),[43] and cucumber basic protein from cucumber seedlings at 1.8 Å resolution (PDB file 2CBP).[46]
45. J. M. Guss, H. D. Bartunik, and H. C. Freeman, *Acta Crystallogr*, 1992, **B48**, 790–807.
46. J. M. Guss, E. A. Meritt, R. P. Phizackerley, and H. C. Freeman, *J. Mol. Biol.*, 1996, **262**, 686–705.